NIH Public Access
Author Manuscript
IEEE Trans Ultrason Ferroelectr Freq Control. Author manuscript; available in PMC 2013 March 27.

Published in final edited form as:
IEEE Trans Ultrason Ferroelectr Freq Control. 2013 March ; 60(3): 451–462. doi:10.1109/TUFFC.2013.2589.

Performance Improvement of Fresnel Beamforming Using Dual Apodization With Cross-Correlation

Man M. Nguyen and **Jesse T. Yen**
The authors are with the University of Southern California, Biomedical Engineering, Los Angeles, CA

Abstract

Fresnel beamforming is a beamforming method that has a delay profile with a shape similar to a physical Fresnel lens. With 4 to 8 transmit channels, 2 receive channels, and a network of single-pole/single-throw switches, Fresnel beamforming can reduce the size, cost, and complexity of a beam-former. The performance of Fresnel beamforming is highly dependent on focal errors resulting from phase wraparound and quantization of its delay profile. Previously, we demonstrated that the performance of Fresnel beamforming relative to delay-and-sum (DAS) beamforming is comparable for linear arrays at f-number = 2 and 50% bandwidth. However, focal errors for Fresnel beamforming are larger because of larger path length differences between elements, as in the case of curvilinear arrays compared with linear arrays. In this paper, we present the concept and performance evaluation of Fresnel beamforming combined with a novel clutter suppression method called dual apodization with cross-correlation (DAX) for curvilinear arrays. The contrast-to-noise ratios (CNRs) of Fresnel beamforming followed by DAX are highest at f-number = 3. At f-number = 3, the experimental results show that using DAX, the CNR for Fresnel beamforming improves from 3.7 to 10.6, compared with a CNR of 5.2 for DAS beamforming. Spatial resolution is shown to be unaffected by DAX. At f-number = 3, the lateral beamwidth and axial pulse length for Fresnel beamforming with DAX are 1.44 and 1.00 mm larger than those for DAS beamforming (about 14% and 21% larger), respectively. These experimental results are in good agreement with simulation results.

I. Introduction

In previous work, we investigated a Fresnel-based beamforming method that has the advantage of reducing channel count from 64 to 128 channels down to 4 to 8 transmit channels and 2 receive channels, thus reducing the number of analog-to-digital converters (ADCs) and time-gain-compensation circuits, and potentially reducing the size, cost, and power of the system. However, the trade-off of this approach is the presence of focal errors, leading to image quality reduction. In the case of linear arrays, these focal errors limit the use of Fresnel beamforming to certain conditions: f-number = 2 and 50% signal bandwidth [1]. Under these conditions, Fresnel beamforming was shown to yield a performance comparable to conventional delay-and-sum (DAS) beamforming. To suppress the effects of focal errors inherent in Fresnel beamforming, we propose the use of dual apodization with cross-correlation (DAX), which is a signal processing method that suppresses side lobes and clutter, thus improving contrast without compromising spatial resolution [2], [3]. In DAX, the received signals are apodized by two aperture functions that have similar main lobes but different side lobe and grating lobe patterns. The two RF data sets are then beamformed and cross-correlated to create a weighting matrix. This weighting matrix is designed so that it passes main-lobe-dominated signals, which have correlation coefficients close to 1, and suppresses clutter-dominated signals, which have correlation coefficients close to or less than 0. In the case of Fresnel beamforming, these aperture functions are assigned as the signals are clustered into 2 receive channels consisting of different sets of elements. Which

NIH-PA Author Manuscript
NIH-PA Author Manuscript
NIH-PA Author Manuscript

NIH-PA Author Manuscript

NIH-PA Author Manuscript

NIH-PA Author Manuscript

channel the signals are passed to is determined by the delay profile of Fresnel beamforming. A curvilinear array was used to evaluate our proposed usage of DAX for Fresnel beamforming for two main reasons. First, because of the curvature, curvilinear arrays have larger path length differences than linear arrays. These differences between curvilinear arrays and linear arrays decrease with deeper focus depths. As an example, in Fig. 1, a curvilinear array with a 40 mm radius of curvature has path length differences at 50 mm depth that are about 2 times larger than a linear array. These larger path length differences lead to higher focusing errors in Fresnel beamforming (Fig. 1), degrading image quality. Therefore, DAX can be used to suppress the side lobes caused by these focusing errors. Second, given the same number of elements and the same pitch, curvilinear arrays have the advantage of an increasing field of view with depth compared with linear arrays [4]. With their trapezoidal shaped field of view, curvilinear array transducers can be used for a wide range of applications such as abdominal or obstetrics and gynecological imaging, or detecting internal bleeding [4]–[8].

In this paper, we propose the integration of DAX with Fresnel beamforming for curvilinear arrays. Spatial resolution and contrast-to-noise ratios are used as image quality metrics. The performance of DAS beamforming is used as the gold standard. This paper is organized as follows: Section II describes Fresnel beamforming along with its benefits and trade-offs, the DAX signal processing method, and the integration of DAX into Fresnel beamforming. Section III presents approaches to evaluate Fresnel beamforming in simulation and experiments. Section IV summarizes our simulation and experimental results using a curvilinear array transducer. The paper concludes with section V.

II. Background

A. Fresnel Beamforming

The goal of beamforming is to focus ultrasound energy at one location. In array transducers, this is achieved by applying time delays or phase shifts corresponding to the path length differences between elements. In Fresnel beamforming, the standard geometric delay Δt is replaced by a new delay Δt_F given by

$$\Delta t_F = \Delta t \bmod T, \quad (1)$$

where mod indicates the modulo operation and T is the period of ultrasound signals based on the center frequency of the transducer. Δt_F is the remainder after integer multiples of the ultrasound period T have been subtracted from Δt [1], [9]. Δt_F is then quantized into equally spaced discrete values. For instance, for a 4-phase Fresnel beamforming, the delay Δt_F has the values of 0, 1/4, 2/4, and 3/4 of the period T, whereas for an 8-phase Fresnel beamforming, Δt_F takes the values from 0 to 7/8 of a period with 1/8 of a period increments. In our design, these time delays Δt_F are implemented using phase shifts. As will be shown later, using 4 and 8 phase shifts allows us to simply utilize inverters and Hilbert transforms to reduce the number of receive channels to 2.

Fig. 1 shows the delay profiles for two 64-element subapertures when geometric focusing is used. These delay profiles are calculated from a curvilinear array with a 40 mm radius of curvature—the same as the array we have available in our lab—and a linear array, both of which focus at a depth of 50 mm. The new delay profiles for Fresnel beamforming are created after integer multiples of the period have been subtracted. These delay profiles have shapes similar to a physical Fresnel lens. Each segment corresponds to a period T, or 360° phase offset. Using Δt_F results in a focal error which is equal to an integer multiple of T plus the error caused by quantization. Focusing errors are plotted in Fig. 1 as the dotted lines. These focal errors will result in higher side lobe levels, higher clutter, and longer pulse

NIH-PA Author Manuscript

NIH-PA Author Manuscript

NIH-PA Author Manuscript

length. Given the same arc length or pitch between elements, the path length differences among elements are larger in curvilinear arrays than in linear arrays because of the convex shape of the curvilinear arrays. This results in twice the number of focal errors for curvilinear arrays as for linear arrays.

1) Fresnel Transmit Beamforming—For a 4-transmit Fresnel system, 4 transmitters are used to generate excitation signals with different time delays corresponding to quarter-period shifts from 0 to 3/4 of a period. Using 4 switches per element, we can control the time delay of a signal emitted by each element (Fig. 2). For an 8-transmit Fresnel system, we will use 8 transmitters to generate signals with 8 different time delays in increments of 1/8 of a period, ranging from 0 to 7/8 of a period.

2) Fresnel Receive Beamforming—Incoming RF signals are subjected to phase shifts based on the delay profile of Fresnel beamforming. A delay in time domain can be transformed into a phase shift in frequency domain using $f(t-\Delta t) \leftrightarrow F(\omega)\, e^{-j\omega\Delta t}$ where $F(\omega)$ is the Fourier transform of $f(t)$. In narrowband applications, the time delay Δt associated with each element can be replaced with an equivalent phase shift that ranges from 0° to 360° based on the following relationship:

$$\theta = -\omega * \Delta t, \quad (2)$$

where ω is the angular central frequency of the transducer [10]. The delay profile is converted into discrete phase shifts that never exceed 360°. When a phase shift greater than 360° is required, the phase shift wraps around and starts back at 0°, introducing focal errors. For example, in the case of a 4-phase Fresnel system, the discrete phase shifts are 0°, 90°, 180°, and 270°, which correspond to the delays of 0, 1/4, 1/2, and 3/4 of a period T, respectively. In broadband applications where (2) is no longer valid, the focal errors become larger, further degrading the performance of Fresnel beamforming relative to conventional DAS beamforming. In fact, Nguyen *et al.* shows that the discrepancies in resolutions between Fresnel beamforming and DAS beamforming decrease as the bandwidth decreases. However, the drawback of narrowband pulses is that they are longer in the time domain, which reduces the axial resolution of ultrasound images—the axial pulse length is approximately doubled when the bandwidth decreases from 50% to 20% [1].

As shown in Fig. 3, four switches per element are used to apply the phase delays to the received signals. The signals with phase shifts of 0°, 90°, 180°, and 270° correspond to switches 1, 2, 3, and 4, respectively. All 0° and 180° phase shifted signals are summed into one receive channel before being digitized by an ADC. In the other receive channel, all 90° and 270° phase shifted signals are summed, digitized by the second ADC, and then phase shifted 90° via a digital Hilbert transform. The resultant data from these 2 channels are then summed digitally to create the beamformed RF data, which can subsequently be envelope detected and log compressed to generate a display image [1].

B. Dual Apodization With Cross-Correlation (DAX)

DAX is a signal processing method that suppresses side lobes and clutter, thus improving contrast without compromising spatial resolution [2], [3]. Assuming linearity, an ultrasound signal is composed of 2 signals: one from the main lobe and one from the side lobes, grating lobes, and other undesirable forms of clutter (other than main lobe). The purpose of DAX is to distinguish side-lobe-dominated signals and minimize their contribution to the image. This approach is achieved by using two receive aperture functions that give similar main lobes and different clutter or side lobe patterns. Some examples of these aperture functions are uniform, Hanning, Hamming, or alternating functions [11], [12]. The signals comprised primarily of main lobe components will have cross-correlation coefficients close to 1,

NIH-PA Author Manuscript

NIH-PA Author Manuscript

NIH-PA Author Manuscript

whereas those comprised mainly of clutter will have cross-correlation coefficients close to or less than 0. A weighting matrix for the beamformed RF data is generated as follows: For each pixel, axial segments of the two real beamformed RF data sets are cross-correlated. If the coefficient is less than a set threshold value $\varepsilon > 0$, that pixel signal is considered side-lobe-dominated and assigned a minimal weighting. This threshold is selected based on the level of decorrelation of the signals that we want to detect and suppress. In yen *et al.* [2], [3], the weighting for side-lobe-dominated signals is set to 0.001, which is equivalent to a 60-dB magnitude reduction. This level of reduction prevents these signals from contributing to the images, normally displayed in a 30 to 50 dB dynamic range [2], [3]. The weighting matrix essentially is the matrix of cross-correlation coefficients after passing through the threshold. The combined, beamformed data are obtained by adding two data sets from the two apertures. If the 2 aperture functions are complementary, i.e., an element is only used in one of the two receive apertures but not in both, the combined data are the same as the data from a standard receive aperture. The combined data are then multiplied with the weighting matrix, envelope detected, and log compressed to generate a display image.

C. Integration of DAX Into Fresnel Beamforming

In the case of Fresnel beamforming, the two receive channels contain RF signals coming from 2 different apertures. These two apertures can be completely complementary in the case of a 4-phase Fresnel system, where the signal from each element is passed to only one of the two channels through a network of switches. Which channel the signals are passed to is determined by the delay profile of Fresnel beamforming and whether the signals require a 0° or 90° phase shift after being digitized. Thus, the apodization functions are dynamically changed with different receive foci. As an illustrative example, Fig. 4 shows a pair of apodization functions at a focus depth of 50 mm. On average, for a 64-element subaperture, there is a slightly higher number of elements in the apodization function for receive channel 1 (34 ± 4 elements) than for receive channel 2 (30 ± 4 elements). These aperture functions have similar main lobe signals and different side lobe signals, and thus DAX can be an approach to distinguish and suppress side lobe signals to improve image contrast.

Fig. 3 shows the receive Fresnel beamforming followed by DAX. Here, the resultant data from two channels will go through ADCs and band-pass filters (BPF1s) with phase shifts. BPF1s band pass the RF signals; first, to isolate the selected frequency range within the transducer bandwidth to construct the image, and second, to filter out signal noise. For our experiment, BPF1s have a 50% bandwidth around the transducer center frequency of 3.3 MH*z.* The data will then be used in two parallel processes. In the first process, the data sets are digitally summed to get the combined, beamformed RF data. In the second process, where DAX is applied, these data sets are used to construct a weighting matrix that can identify and suppress side-lobe-dominated signals. Because of the inherent focal errors in Fresnel beamforming when used with broadband signals, the side lobes of Fresnel beamforming are higher than those of DAS, which reduces image contrast. These side lobe levels increase as the signal bandwidth increases because of increasing focal errors from the violation of the narrowband assumption [1]. This correlated attribute of these side lobes can limit the capability of DAX to identify and suppress them. However, with another set of narrow band-pass filters (BPF2s) to reduce focal errors caused by the violation of the narrowband assumption, this correlation attribute of the side lobes can be reduced, thus allowing side-lobe-dominated signals to be better distinguished and suppressed by DAX. As a trade-off, the axial pulse length becomes longer as the signal bandwidth decreases. The elongation of axial pulse can increase the correlation between signals above and below the cyst and the side-lobe-dominated signals inside the cyst. This limits the efficiency of side lobe suppression using DAX. Because axial pulse length and side lobe levels both affect

NIH-PA Author Manuscript

NIH-PA Author Manuscript

NIH-PA Author Manuscript

CNR, an optimal bandwidth for BPF2s must be determined to maximize CNRs. In our study, the optimal –6-dB fractional bandwidth for BPF2s was empirically found to be 15%.

After being filtered by BPF2s, the resultant data sets are then cross-correlated. The matrix of cross-correlation coefficients subsequently passes through a threshold and functions as a weighting matrix. Finally, a DAX-applied image is obtained after the beamformed RF data are multiplied with this weighting matrix, envelope detected, and log compressed.

III. Methods

We investigate the performance of Fresnel beamforming with and without DAX in terms of spatial resolution and CNR. Without DAX, the higher number of focal errors for a curvilinear array compared with a linear array potentially results in higher side lobe levels, higher clutter, and longer pulse length for Fresnel beamforming. However, by applying DAX, we expect to reduce the amount of clutter and lower side lobe levels without compromising lateral beamwidth and axial pulse length. To quantify the performance, we have performed simulations and experiments to evaluate our proposed integration of DAX into Fresnel beamforming for curvilinear arrays.

A. Simulations

We performed Field II simulation to evaluate the performance of Fresnel beamforming on a curvilinear array with and without DAX [13]. The lateral beamwidth and axial pulse lengths of Fresnel beamforming were examined with different f-numbers. The results of Fresnel beamforming were then compared with those of DAS, which served as the gold standard. A 3.3-MHz Gaussian pulse with 50% bandwidth was used as the transmit pulse.

B. Experimental Setup

For our experimental setup, full synthetic aperture RF data sets were collected and sampled at 20 MHz, using Verasonics Data Acquisition System (VDAS; Verasonics Inc., Redmond, WA) with an ATL C4–2 curvilinear array (Philips ATL, Bothell, MA). This 128-element array has a radius of 40 mm and an aperture angle of 75°. The data was then beam-formed offline with DAS beamforming and the proposed Fresnel focusing techniques. For the Fresnel beamforming techniques, the transmit delays applied to the signals only take 4 values, ranging from 0 to 3/4 of a period T(1). These delay values were implemented in Matlab (The MathWorks Inc., Natick, MA) by delaying the signals in terms of samples. On receive, the signals are subjected to 0°, 90°, 180°, 270° phase shifts, which can be implemented offline by multiplying the signals with −1 and/or Hilbert transform. The performance of Fresnel beamforming with and without DAX was evaluated in terms of spatial resolution and CNR. The robustness of Fresnel beamforming was also assessed by using f-numbers ranging from 2 to 4. The lateral beam spacing is 0.14°, which results in a 0.225 mm lateral beam spacing at 50 mm depth. The transmit focusing was fixed at 50 mm, which is at the center of the cyst and wire targets, whereas the dynamic receive focusing was updated every 1 mm.

Table I presents the parameters used for Field II simulation and experimental setup. The pitch, element height, radius of curvature, aperture angle, and center frequency were chosen to match the aTl C4–2 curvilinear array transducer. The sound speed of 1480 m/s, which is that of water, was used in simulation, providing a better context for relating our simulation results and experimental results.

1) Spatial Resolution—We imaged a 0.05-mm-diameter human hair target immersed at 50 mm depth in degassed water. The full synthetic data set was collected within two hours

NIH-PA Author Manuscript

NIH-PA Author Manuscript

NIH-PA Author Manuscript

after the hair was submerged in water. The –6-dB lateral and axial target sizes were measured to serve as metrics for spatial resolution.

2) Contrast-to-Noise Ratio (CNR)—A full synthetic aperture RF data set of an ATS ultrasound phantom (Model 539, ATS Laboratories, Bridgeport, CT) containing a 6-mm-diameter cylindrical anechoic cyst at 50 mm depth was collected. The data was then beamformed with offline DAS beamforming and the proposed Fresnel focusing techniques. CNR is defined as the difference between the mean of the background (the area surrounding the cyst) and the cyst in decibels, divided by the standard deviation of the background in decibels (after beamforming and log compression) [14]:

$$\mathrm{CNR}=\frac{\bar{S}_{\mathrm{t}}-\bar{S}_{\mathrm{b}}}{\sigma_{\mathrm{b}}}, \quad (3)$$

where $\bar{S}_{\mathrm{t}}$ is the mean of the signal amplitude from the target (in decibels), $\bar{S}_{\mathrm{b}}$ is the mean of the signal amplitude coming from the background (in decibels), and σ_{b} is the standard deviation of the signal amplitude from the background (in decibels).

Using the VDAS, we used a sampling frequency of 20 MHz for our experiments. At this frequency, signals of a 3.3-MHz transducer are sampled at a rate of 6 samples per wavelength. The delays applied to the 4 transmitters ideally are 0, 1/4, 1/2, and 3/4 of a period, which are equivalent to 0, 1.5, 3, and 4.5 samples. Without interpolation, instead of having a 3- or 6-transmitter Fresnel system, we implemented Fresnel beamforming with 4 transmitters which have unequally spaced delays of 0, 1, 3, and 4 samples to preserve the same number of switches and transmitters of the system. By comparing with a system with equally spaced delay transmitters, we found that the additional focal errors caused by unequally spaced delays have minor effects on Fresnel beamforming, with less than 2% discrepancies in terms of CNR and resolution. Furthermore, this sampling rate of 6 samples per wavelength does not affect the receive side of a 4 or 8-phase Fresnel beamforming, where phase shifts are applied.

As described earlier, there are several parameters in the DAX algorithm that can be adjusted to provide the optimal performance of the system when DAX is combined with Fresnel beamforming. These parameters include the threshold for the cross-correlation matrix, the size of median filter, the segment length for cross-correlation, and the band-pass filter used for DAX. By varying these parameters, the values in Table II empirically provide the best performance in terms of CNR for Fresnel beamforming with DAX.

IV. Results and Discussion

A. Simulation Results

Fig. 5 shows the effect of f-number on the performance of 4-phase and 8-phase Fresnel beamforming methods compared with delay-and-sum (DAS), without dual apodization with cross-correlation (DAX) [Figs. 5(a) and 5(b)] and with DAX [Figs. 5(c) and 5(d)]. Applying DAX minimally affects the spatial resolution of Fresnel beamforming with the largest differences being 0.03 mm for axial pulse length and 0.08 mm for lateral beamwidths. This is expected because DAX was shown to suppress the side lobes without broadening the main lobes [2], [3]. With DAX, as the f-number increases from 2 to 4, the −6-dB lateral beamwidth also increases. For example, the lateral beamwidth changes from 1.06 to 1.50 mm for 4-phase Fresnel beamforming, from 1.18 to 1.46 mm for 8-phase Fresnel beamforming, and from 0.90 to 1.57 mm for DAS beamforming, as shown in Fig. 5(c). As the f-number increases, the discrepancies in lateral beamwidth between Fresnel and DAS

NIH-PA Author Manuscript

NIH-PA Author Manuscript

NIH-PA Author Manuscript

beamforming also decrease, from 0.28 mm at f-number = 2 to 0.11 mm at f-number = 4 for 8-phase Fresnel beamforming for example. Furthermore, the discrepancies in axial pulse length between Fresnel and DAS beamforming also decrease from about 1.3 mm to 0.1 mm as the f-number increases from 2 to 4 [Figs. 5(b) and 5(d)]. To clarify, the axial pulse length for 8-phase Fresnel beamforming with DAX decreases from 1.92 mm at f-number = 2 to 0.71 mm at f-number = 4, approaching the axial pulse length of 0.59 mm for DAS beamforming with DAX.

The decreasing discrepancies in spatial resolution between Fresnel and DAS beamforming with increasing f-numbers can be explained by the decreasing number of focal errors in Fresnel beamforming. In fact, the maximum path length difference between outer and center elements is reduced from 6 wavelengths to 2 wavelengths as f-number goes from 2 to 4. This results in a maximum focal error of 1 wavelength for Fresnel beamforming at f-number = 4 as shown in Fig. 1.

Fig. 6 shows the lateral beamplots simulated with Field II, using DAS and 4-phase Fresnel beamforming with and without DAX at f-number = 2 [Fig. 6(a)], 3 [Fig. 6(b)] and 4 [Fig. 6(c)]. Even though the main lobe beamwidths for Fresnel beamforming are comparable with those for DAS, the side lobe levels for Fresnel beamforming are about 6 to 15 dB higher than those for DAS, which can degrade image contrast. As the f-number increases, these side lobe levels of Fresnel beamforming become lower as a result of smaller focal errors. In the case of 4-phase Fresnel beamforming, the side lobe level is decreased from −9 dB at f-number = 2 to −20 dB at f-number = 4. Using DAX, signals away from the main lobe are more suppressed than the ones near the main lobe. For instance, at f-number = 2, the clutter at a lateral distance of 2 mm away from the main lobe is suppressed from −17 dB to −21 dB, whereas the clutter at a lateral distance of 4 mm away from the main lobe is suppressed from −26 dB to −51 dB. These effects are seen later in experimental single-wire images (Figs. 7 and 8).

B. Experimental Results

1) Spatial Resolution—Figs. 7 and 8 show the experimental images of a target of human hair, using the three different beamforming techniques without DAX (Fig. 7) and with DAX (Fig. 8) in a 60 dB dynamic range. As seen in Fig. 7, the clutter in Fresnel beamforming becomes less noticeable, with the trade-off of enlarging lateral beamwidths as the f-number increases. The clutter, especially beyond 3 mm laterally away from the main beam, is suppressed with DAX, as shown in Fig. 8. These results agree with the simulated results, where the clutter in these regions is suppressed by about 20 dB.

Fig. 9 quantifies the plots of experimental lateral beamwidths and axial pulse lengths against f-numbers without DAX [Figs. 9(a) and 9(b)] and with DAX [Figs. 9(c) and 9(d)]. Similar to the simulated results, these results show that applying DAX does not affect spatial resolution, with a maximum difference of 0.02 mm for lateral beamwidths. This maximum difference is 0.07 mm for axial pulse length. Regarding spatial resolution of Fresnel beamforming, the same trends are seen in experimental results as in simulation results. As the f-number increases from 2 to 4, the −6-dB lateral beamwidth enlarges from 1.38 to 1.69 mm for 4-phase Fresnel beamforming, and from 1.24 to 1.66 mm for 8-phase Fresnel beamforming. The axial pulse length decreases from 1.92 to 0.83 mm for 4-phase Fresnel beamforming, and from 1.89 to 0.84 mm for 8-phase Fresnel beamforming. The resolution of Fresnel beamforming and DAS beamforming also converges to within a 5% discrepancy as the f-number increases to 4, where the focal errors are reduced to about 1 wavelength.

2) Contrast-to-Noise Ratio—Fig. 10 shows the experimental images of 6-mm-diameter cylindrical anechoic cysts in the ATS tissue mimicking phantom. Here, the clutter inside the

NIH-PA Author Manuscript

NIH-PA Author Manuscript

NIH-PA Author Manuscript

cyst and the noncircular shape of the cyst in the images for Fresnel beamforming are the results of high side lobe levels resulting from focal errors, as seen in Figs. 6–8. As the f-number increases, the cyst appears more circular with less clutter. In fact, the CNRs increase from 3.0 at f-number = 2 to 3.8 at f-number = 4 for 4-phase Fresnel beamforming, and from 3.0 to 3.9 for 8-phase Fresnel beamforming, approaching CNRs for DAS beamforming.

Fig. 11 shows the experimental images of the same cysts with DAX applied. Shown in the same dynamic range of 40 dB as those in Fig. 10, these cysts appear darker with less clutter. These visual improvements are quantified with the CNR measurements, which have improved by at least 100%. For example, applying DAX on DAS beamforming improves the CNR from 5.2 to 11.2 at f-number = 3, and from 4.9 to 11.4 at f-number = 4. For 4-phase Fresnel beamforming, the CNRs are improved from 3.7 to 10.6 at f-number = 3, and from 3.8 to 9.1 at f-number = 4. These improvements are expected because of the reduction of side lobe levels when DAX is applied, as previously shown in Fig. 6.

Fig. 12 summarizes the plots of CNRs against different f-numbers for DAS and Fresnel beamforming with and without DAX. As the f-number increases from 2 to 4, the CNRs for Fresnel beamforming without DAX slightly improve slightly from 3.0 to 3.8, approaching the CNRs for DAS beamforming, which decreases from 5.3 to 5.0. This is expected as a result of the decreasing side lobe levels in Fresnel beamforming. The CNRs are also compatible within 10% for 4-phase and 8-phase Fresnel beamforming across all f-numbers. The CNRs of Fresnel beamforming with DAX are highest at f-number = 3, where CNRs for 4-phase Fresnel with DAX and 8-phase Fresnel with DAX are 10.6 and 10.9. These CNRs are 5.2% and 2.4% lower than the CNR of 11.2 from DAS beamforming with DAX, respectively. F-number = 3 is also the point where the spatial resolution for Fresnel beamforming is comparable with those of DAS (Figs. 5 and 9).

V. Conclusion and Future Work

In this paper, we presented the concept and performance evaluation of Fresnel beamforming followed by DAX for curvilinear array transducers. The Fresnel beamforming technique allows a system with 4 to 8 transmit channels and 2 receive channels with a network of single-pole/single-throw switches to focus an array. It is shown that combining DAX with Fresnel beamforming can result in 4 to 20 dB of clutter suppression, and at least a 100% improvement in CNR. Therefore, the proposed integration of DAX into Fresnel beamforming suppresses the effects of focal errors in Fresnel beamforming, allowing it to be used in curvilinear arrays. In fact, even though the results shown in this paper come from a curvilinear array with the radius of 40 mm, similar analysis can be used for arrays with different radii. For instance, the performance of Fresnel beamforming is expected to improve for curvilinear arrays with larger radii as a result of decreasing focal errors. On the other hand, bigger f-numbers may be needed to reduce the number of focal errors for arrays with smaller radii.

The experimental results show that using Fresnel beamforming with DAX results in CNRs that are at least 40% higher than those from traditional DAS beamforming. The optimal CNR using Fresnel beamforming with DAX occurs at f-number = 3, where the CNRs for 4- and 8-phase Fresnel beamforming with DAX are, respectively, 104% and 109% higher than the CNR of 5.2 for DAS beamforming alone. F-number = 3 is also the point where spatial resolution for Fresnel beamforming with DAX becomes comparable with DAS beamforming. At f-number = 3, the experimental lateral beamwidth and axial pulse length for 8-phase Fresnel beamforming with DAX are 1.44 and 1.00 mm, respectively, which are about 14% and 21% larger than those for DAS beamforming. One possible explanation for the decreasing CNRs of Fresnel beamforming with DAX for f-numbers greater than 3 is the

NIH-PA Author Manuscript

NIH-PA Author Manuscript

NIH-PA Author Manuscript

decreasing effectiveness of the narrowband filters (BPF2s) in reducing the correlation of side lobes for two receive apodizations. The performance of 4-phase and 8-phase Fresnel beamforming are comparable for axial pulse length to within a 2% discrepancy, and for both lateral beamwidth and CNR to within 10%. Although 8-phase Fresnel beamforming uses twice as many time delays and phase shifts as 4-phase Fresnel beamforming does, the implementation of some phase-shifted signals in 8-phase Fresnel beamforming are not sufficient. For example, 45° phase shift is implemented by adding 0° and 90° phase-shifted signals. This implementation also results in a 3 dB increase in signal magnitude [1].

Instead of using 64 to 128 channels with one ADC for each channel, our proposed Fresnel beamforming uses a total of two ADCs. The number of time-gain-compensation (TGC) circuits can also be reduced by placing the TGC circuits after the inverting/noninverting summing amplifiers. For Fresnel beamforming, transmit/receive (T/R) switches will go between the inverting/noninverting amplifiers and each phase-shifted clustering signal. Because there are four clustering signals (0°, 90°, 180°, and 270° phase shifted), four T/R switches are needed. Although a standard beamformer usually has fewer multiplexers than elements, a Fresnel beamformer has the same number of high-voltage multiplexers as the number of elements. In a beamformer, ADCs are considered the most expensive, and consume the most power and room [15]. Therefore, the benefits of reducing the number of channels and ADCs will likely outweigh the drawbacks of increasing the number of switches, resulting in a reduction in the cost, power, and size of the system. The delays of receive signal can be applied in real time with the adjustments of the switches in Fresnel beamformer. Furthermore, DAX is a computational signal processing method that does not require additional components in the beamformer. It can be run in parallel with the beamformer, allowing real-time imaging. However, one possible drawback of using multiple switches is that glitches from the switches could create issues in hardware implementation. Therefore, we selected switches with low capacitance and charge injection, which are good for low glitch and fast settling.

Apodization functions, including Hanning, Hamming, or constrained least squares, can be used to suppress the side lobe levels at the cost of widening main lobe beamwidths [11], [12], [16]. For example, Hanning apodization lowers side lobe levels from −26 to −57 dB at the cost of widening −6-dB main lobe beamwidths by approximately one half [2]. These apodization functions can also help to reduce side-lobe levels in Fresnel beamforming, especially when the weights of the outer elements are smaller. However, although it is possible to use different apodization functions for DAS, other apodization functions besides those inherent in the two Fresnel receive channels will increase the complexity, as well as the number of transmits per frame in Fresnel beamforming, thus reducing frame rate [1]. Therefore, a uniform apodization was used for DAS without DAX as a baseline for investigating the effects of focal errors in Fresnel beamforming and the effectiveness of DAX when combined with Fresnel beamforming. Similarly, the same apodization functions were used for Fresnel beamforming with DAX and for DAS beamforming with DAX to maintain consistency. In fact, these apodization function pairs are similar to a randomly selected aperture pair presented in Yen *et al.*, which underperforms an apodization pair of alternating patterns by about 12% in terms of CNR around the focus [2]. However, the variations of these inherent apodization functions along receive foci reduce the artifacts (black spots) away from the transmit focus. In Yen *et al.*, these artifacts were suppressed using different pairs of apodization functions at different depths [3].

Although Fresnel beamforming with DAX has CNRs that are at least 40% larger than traditional DAS beamforming, the noncircular appearance of cylindrical anechoic cysts can be an issue. In some applications, the shape of a cyst can be a critical factor in the treatment plan for a patient, such as discerning benign versus malignant tissues in diagnostic imaging.

NIH-PA Author Manuscript

NIH-PA Author Manuscript

NIH-PA Author Manuscript

This noncircularity is likely an effect of focal errors of Fresnel beamforming and requires further signal processing to be removed. However, for applications in which detectability rather than classification is the main objective, such as internal bleeding or lesion detection, Fresnel beamforming followed by DAX may be a suitable alternative for ultrasound systems with curvilinear arrays.

In conclusion, Fresnel beamforming with DAX is shown to have higher CNR and spatial resolution comparable to DAS beamforming for curvilinear arrays. With the advantage of reducing channel count from 64 to 128 channels down to 4 to 8 transmit channels and 2 receive channels, Fresnel beamforming with DAX can help to reduce the cost and size of ultrasound systems with curvilinear arrays. Future work includes investigating other efficient signal processing methods to eliminate the noncircular shape of the cyst and developing a prototype imaging device.

References

[1]. Nguyen M, Mung J, Yen J. Fresnel-based beamforming for low-cost portable ultrasound. IEEE Trans. Ultrason. Ferroelectr. Freq. Control. 2011; 58(1):112–121. [PubMed: 21244979]

[2]. Seo C, Yen JT. Sidelobe suppression in ultrasound imaging using dual apodization with cross-correlation. IEEE Trans. Ultrason. Ferroelectr. Freq. Control. 2008; 55(10):2198–2210. [PubMed: 18986868]

[3]. Seo C, Yen JT. Evaluating the robustness of dual apodization with cross-correlation. IEEE Trans. Ultrason. Ferroelectr. Freq. Control. 2009; 56(2):291–303. [PubMed: 19251516]

[4]. Whittingham, T.; Martin, K. Transducer and beamforming. In: Hoskins, P.; Martin, K.; Thrush, A., editors. Diagnostic Ultrasound: Physics and Equipment. Cambridge University Press; New York, NY: 2010. p. 23-46.

[5]. Thijssen JM, Starke A, Weijers G, Haudum A, Herzog K, Wohlsein P, Rehage J, De Korte CL. Computer-aided B-mode ultrasound diagnosis of hepatic steatosis: A feasibility study. IEEE Trans. Ultrason. Ferroelectr. Freq. Control. 2008; 55(6):1343–1354. [PubMed: 18599422]

[6]. Kirkpatrick AW, Šustic A, Blaivas M. Introduction to the use of ultrasound in critical care medicine. Crit. Care Med. 2007; 35(5):123–125.

[7]. Iwashita T, Nakai Y, Lee JG, Park DH, Muthusamy VR, Chang KJ. Newly-developed, forward-viewing echoendoscope: A comparative pilot study to the standard echoendoscope in the imaging of abdominal organs and feasibility of endoscopic ultrasound-guided intervention. J. Gastroenterol. Heptaol. 2012; 27(2):362–367.

[8]. Bushberg, JT.; Seibert, JA.; Leidholdt, ED.; Boone, JM. The Essential Physics of Medical Imaging. 2nd ed.. Lippincott Williams & Wilkins; Philadelphia, PA: 2000.

[9]. Richard, B.; Fink, M.; Alais, P. New arrangements for Fresnel focusing. In: Wang, K., editor. Acoustical Imaging. Vol. vol. 9. Plenum Press; New York, NY: 1980. p. 65-73.

[10]. Rudnick P. Digital beamforming in the frequency domain. J. Acoust. Soc. Am. 1969; 46(5A): 1089–1090.

[11]. Wang, H. System and method for adaptive beamformer apodization. U.S. Patent 6 436 044. Aug.. 2002

[12]. Stankwitz HC, Dallaire RJ, Fienup JR. Nonlinear apodization for side lobe control in SAR imagery. IEEE Trans. Aerosp. Electron. Syst. 1995; 31(1):23–52.

[13]. Jensen JA, Svendsen JB. Calculation of pressure fields from arbitrarily shaped, apodized, and excited ultrasound transducers. IEEE Trans. Ultrason. Ferroelectr. Freq. Control. 1992; 39(2): 262–267. [PubMed: 18263145]

[14]. Krishnan S, Rigby KW, O'Donnell M. Improved estimation of phase aberration profile. IEEE Trans. Ultrason. Ferroelectr. Freq. Control. 1997; 44(3):701–713.

[15]. Lee H, Sodini CG. Analog-to-digital converters: Digitizing the analog world. Proc. IEEE. 2008; 96(2):323–334.

NIH-PA Author Manuscript

NIH-PA Author Manuscript

NIH-PA Author Manuscript

[16]. Guenther DA, Walker WF. Optimal apodization design for medical ultrasound using constrained least squares Part II: Simulation results. IEEE Trans. Ultrason. Ferroelectr. Freq. Control. 2007; 54(2):343–358. [PubMed: 17328331]

NIH-PA Author Manuscript
NIH-PA Author Manuscript
NIH-PA Author Manuscript

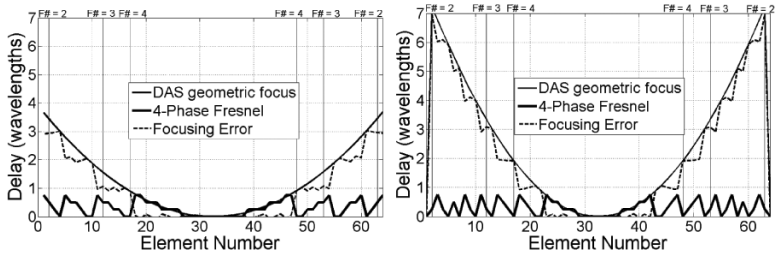

Fig. 1.

An example of delay profiles of Fresnel beamforming and focusing errors in terms of wavelength for a 64-element subaperture of a linear array (left) and a curvilinear array (right). In both profiles, the focused point is set at a depth of 50 mm. The curvilinear array has a 40 mm radius of curvature. Vertical lines indicate the range of elements that are used for specific f-numbers.

NIH-PA Author Manuscript

NIH-PA Author Manuscript

NIH-PA Author Manuscript

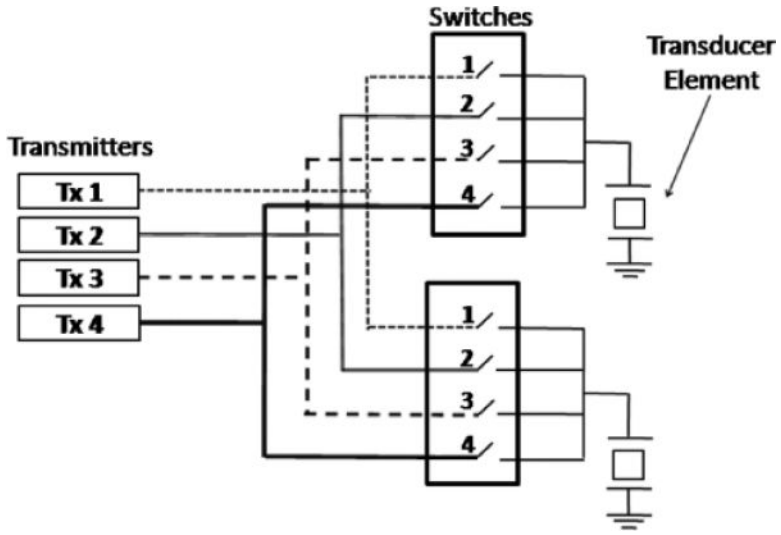

Fig. 2.
A 4-transmit Fresnel beamforming schematic diagram for a 2-element array [1].

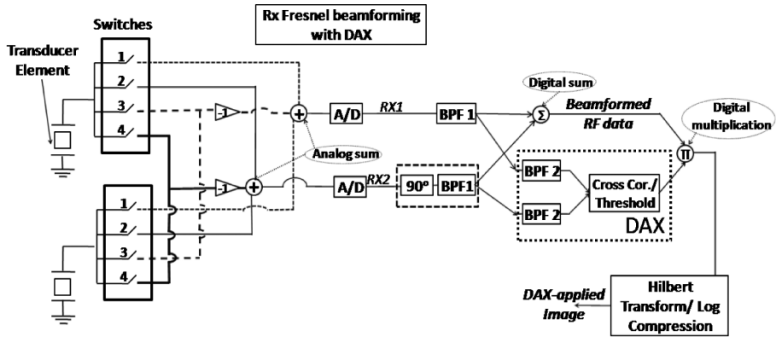

Fig. 3.

Fresnel beamforming schematic diagram for a 2-element array combined with dual apodization with cross-correlation (DAX). 0° phase shift is applied by closing switch 1, 45° by closing switch 1 and 2, 90° by closing switch 2. Inverting amplifiers are used with switches 3 and 4 to obtain 180° and 270° phase shifts, respectively. The signals will go through two receiving channels, each of which has an A/D converter and a digital band-pass filter (BPF). BPF2s have a narrow bandwidth and are used in generating DAX weighting matrix.

NIH-PA Author Manuscript NIH-PA Author Manuscript NIH-PA Author Manuscript

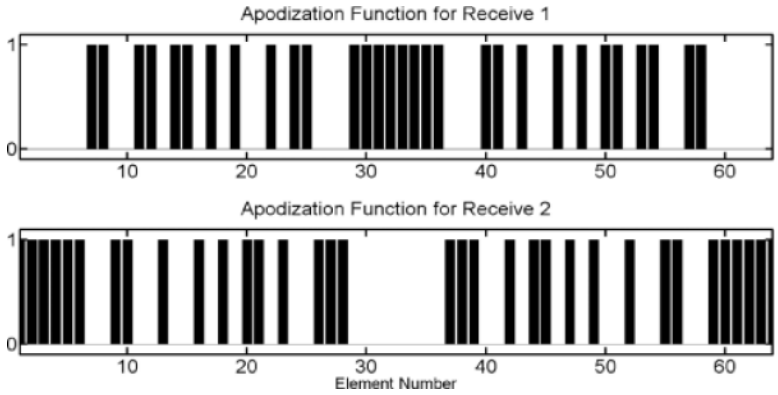

Fig. 4.
Pair of receive subapertures in Fresnel beamforming at 50 mm depth.

NIH-PA Author Manuscript
NIH-PA Author Manuscript
NIH-PA Author Manuscript

NIH-PA Author Manuscript

NIH-PA Author Manuscript

NIH-PA Author Manuscript

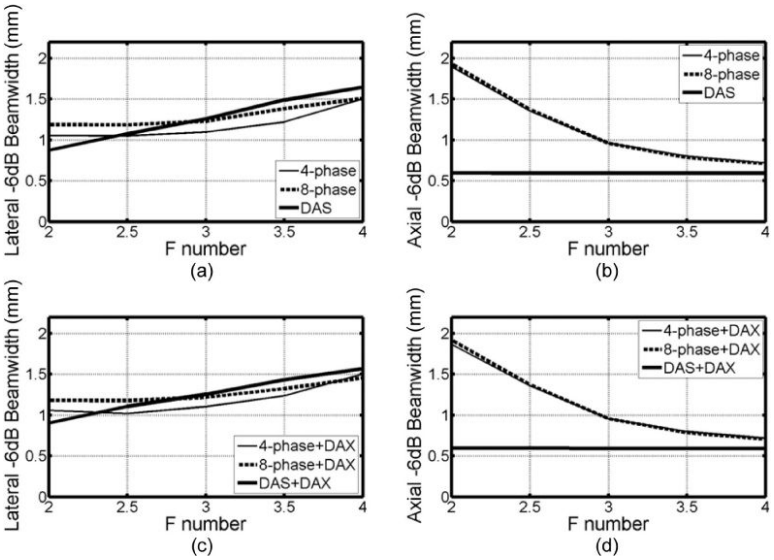

Fig. 5.

Simulated spatial resolution of 3 beamforming algorithms (a and b) without dual apodization with cross-correlation (DAX) and (c and d) with DAX. The signal bandwidth is 50%.

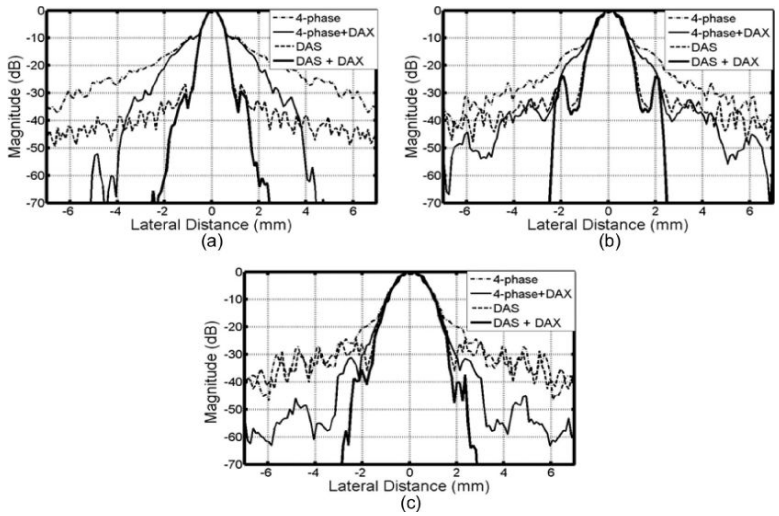

Fig. 6.

Simulated lateral beamplots using delay-and-sum (DAS), 4-phase Fresnel beamforming with and without dual apodization with cross-correlation (DAX) at f-number of (a) 2, (b) 3, and (c) 4. The side lobe levels of Fresnel beamforming decrease with higher f-numbers. Applying DAX is shown to reduce these side lobe levels without affecting the main lobe beamwidth.

NIH-PA Author Manuscript
NIH-PA Author Manuscript
NIH-PA Author Manuscript

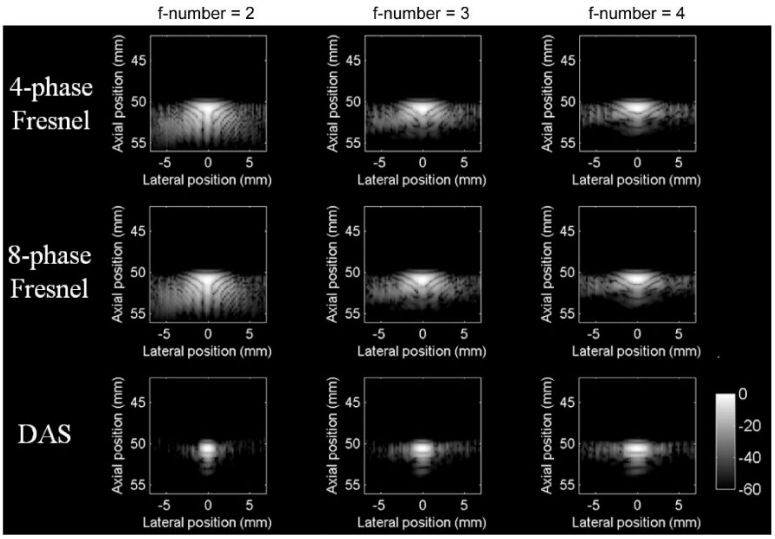

Fig. 7.

Experimental single-wire images without dual apodization with cross-correlation (DAX) using 4-phase Fresnel, 8-phase Fresnel, and delay-and-sum (DAS) with 50% signal bandwidth and f-numbers of 2, 3, and 4.

NIH-PA Author Manuscript
NIH-PA Author Manuscript
NIH-PA Author Manuscript

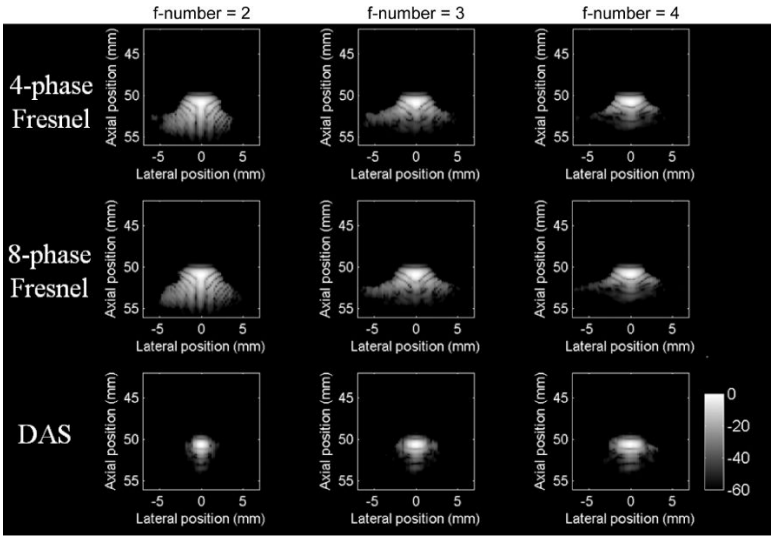

Fig. 8.

Dual apodization with cross-correlation (DAX)-applied experimental single-wire images using 4-phase Fresnel, 8-phase Fresnel, and delay-and-sum (DAS) with 50% signal bandwidth and f-numbers of 2, 3, and 4.

NIH-PA Author Manuscript
NIH-PA Author Manuscript
NIH-PA Author Manuscript

NIH-PA Author Manuscript

NIH-PA Author Manuscript

NIH-PA Author Manuscript

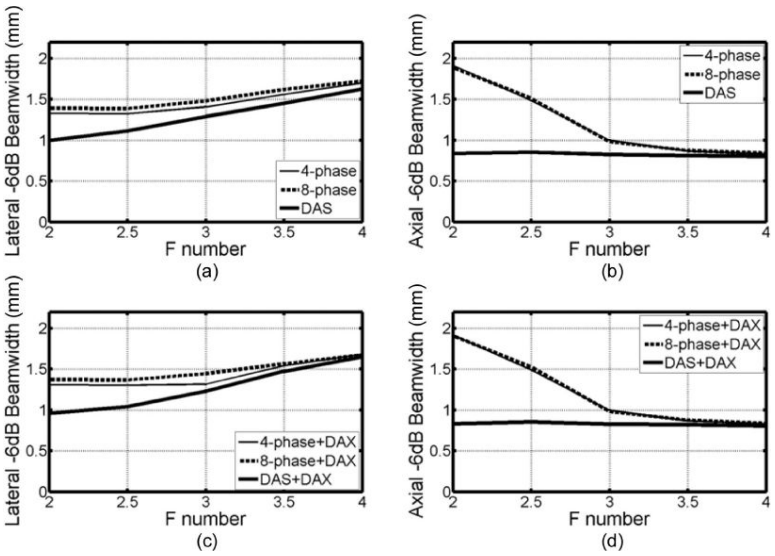

Fig. 9.

Experimental spatial resolution of 3 beamforming algorithms (a and b) without dual apodization with cross-correlation (DAX) and (c and d) with DAX. The signal bandwidth is 50%.

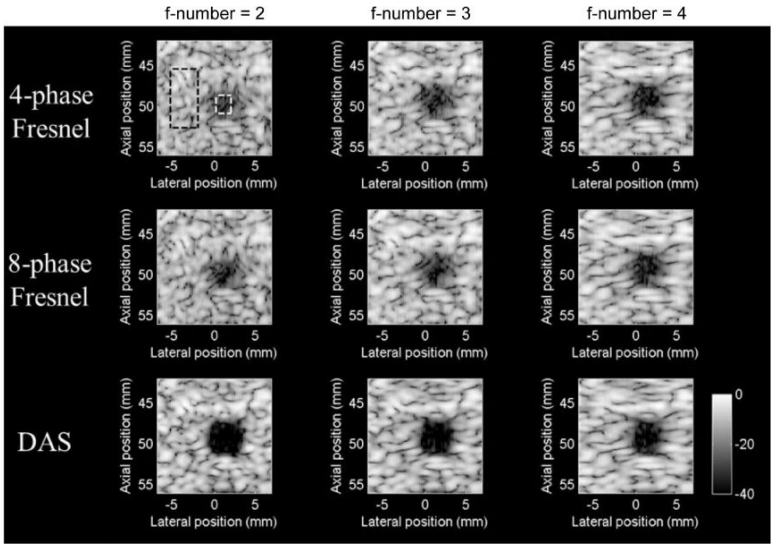

Fig. 10.

Experimental 6-mm-diameter cylindrical cyst images without dual apodization with cross-correlation (DAX) using 4-phase Fresnel, 8-phase Fresnel, and delay-and-sum (DAS) beamforming with 50% signal bandwidth and f-numbers of 2, 3, and 4.

NIH-PA Author Manuscript
NIH-PA Author Manuscript
NIH-PA Author Manuscript

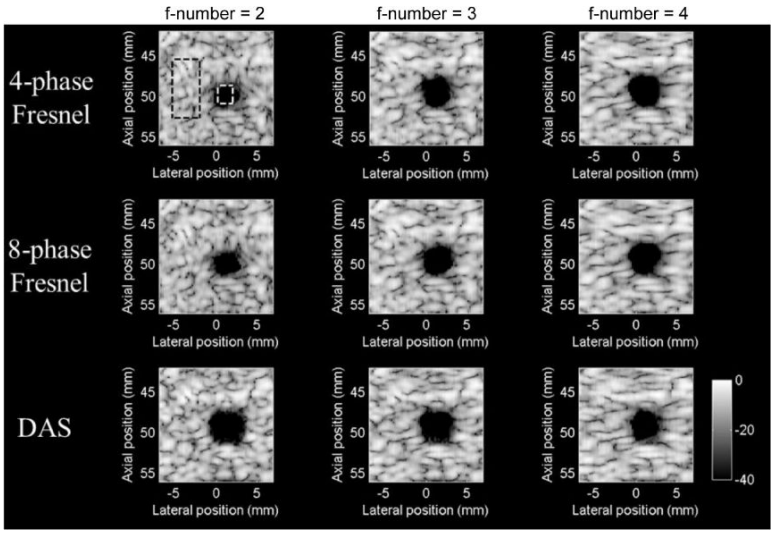

Fig. 11.

Dual apodization with cross-correlation (DAX)-applied experimental 6-mm-diameter cylindrical cyst images using 4-phase Fresnel, 8-phase Fresnel, and delay-and-sum (DAS) beamforming with 50% signal bandwidth and f-numbers of 2, 3, and 4.

NIH-PA Author Manuscript
NIH-PA Author Manuscript
NIH-PA Author Manuscript

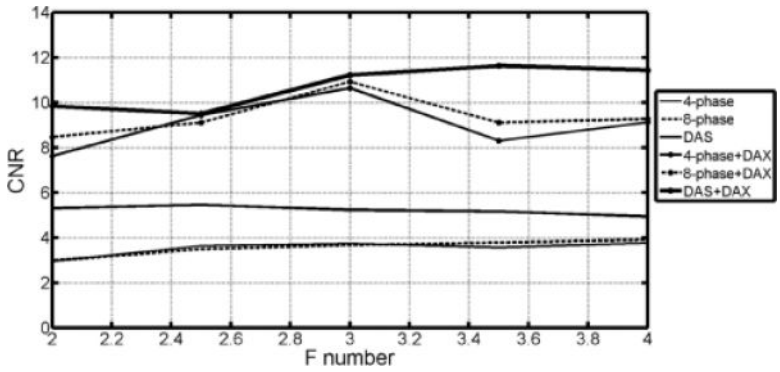

Fig. 12.

Experimental comparison of beamforming methods in terms of contrast-to-noise ratio (CNR): 4-phase Fresnel, 8-phase Fresnel, and delay-and-sum (DAS) with and without dual apodization with cross-correlation (DAX) applied.

NIH-PA Author Manuscript NIH-PA Author Manuscript NIH-PA Author Manuscript

NIH-PA Author Manuscript

NIH-PA Author Manuscript

NIH-PA Author Manuscript

TABLE I

Parameters for Simulation and Experimental Setup.

Parameter	Value
Radius of curvature	40 mm
Aperture angle	75°
Center frequency	3.3 MHz
Sampling frequency	20 MHz
Azimuthal element pitch	0.409 mm
Elevation element height	13 mm
Sound speed	1480 m/s (water)
	1450 m/s (phantom)
Transmit focus	50 mm
Lateral beam spacing	0.14° (0.225 mm at 50 mm depth)
Receive focal delay step	1 mm

NIH-PA Author Manuscript

NIH-PA Author Manuscript

NIH-PA Author Manuscript

TABLE II

DAX Parameters for Experimental Setup.

Parameter	Value
Threshold	0.001
Cross-correlation segment size	6 samples
Median filter size	$4\lambda \times 4\lambda$
Filter bandwidth (BPF2)	15%